SSRG International Journal of Electrical and Electronics Engineering
ISSN: 2348-8379/ https://doi.org/10.14445/23488379/IJEEE-V13I1P114

Volume 13 Issue 1, 142-153, January 2026

Original Article

Channel Estimation and Optimal Power Allocation using Adaptive Optimizer in Cell Free Massive MIMO-NOMA

V Satya Kumar Kudipudi[1], S. Neeraja[2]

[1,2]*Department of EECE, GITAM (Deemed to be University), Visakhapatnam, India.*

[1]*Corresponding Author : k.v.satyakumar@gmail.com*

Received: 08 November 2025 Revised: 10 December 2025 Accepted: 09 January 2026 Published: 14 January 2026

Abstract *- Non-Orthogonal Multiple Access (NOMA) is considered as one of the emerging multi-access technologies for 5G communication, and also can enhance the system's performance. It is integrated with Cell-Free Massive Multiple Input Multiple Output (CF-MA-MIMO) to support multiple users, producing a high gain. Optimizing spectral and energy efficiencies is a challenging process due to the non-linear programming involved. The proposed model considered the downlink transmission of the Cell Free-Massive-Multiple Input Multiple Output- Non-Orthogonal Multiple Access (CF- MA-MIMO-NOMA). This work presents an enhanced approach for channel estimation and optimal power allocation in CF- MA-MIMO-NOMA. Initially, the user equipment estimates the channels for every user and then provides them to the MA-MIMO. Then, the Expectation Maximization (EM) is utilized for Channel Estimation (CE), and the metaheuristic algorithm Adaptive Squirrel Search Optimization (ASSO) is utilized for optimal power allocation. The proposed ASSO attained better spectral efficiency, energy efficiency, and sum rate by the power allocation at the different users and SNR values.*

Keywords *- Cell Free-Massive-Multiple-Input Multiple-Output, Non-Orthogonal Multiple Access, Expectation Maximization, Adaptive Squirrel Search Optimization.*

1. Introduction

Due to the development of emerging applications, there is a demand for ultra-high-speed connections for upcoming wireless communication. In the year 2020, there are approximately 20 billion devices linked to the Internet, and by the year 2025, it is predicted that it may exceed 23 billion devices [1, 2]. The conventional Orthogonal Multiple Access (OMA) approaches are reaching the fundamental limits, and they are not able to fulfill further requirements. NOMA is an emerging solution that increases the Spectral Efficiency (SE), Energy Efficiency (EE), and user fairness of Conventional Communications [3]. In NOMA, multiple User Equipment (UE) are utilized for transmitting and receiving the signals simultaneously using time, frequency, and code domains. Massive-Multiple Input Multiple Output (MA-MIMO) is an efficient model utilized in wireless communication, and it attains better bandwidth and maximum SE [4-6]. In MA-MIMO systems, different antennas are employed on the transmitter as well as the receiver side. In the MIMO system, each antenna exploits the Radio Frequency (RF) chain to realize the processing of the signal in the digital format [7]. The MA-MIMO utilizes multiple RF chains to utilize excessive energy. NOMA achieves significant outcomes in the multi-access issues and satisfies the needs of 5G and 6G networks. Furthermore, it enhances the quality of service (Quality of Service), such as SE and mass connectivity [8]. The primary aim of the NOMA is to exploit the power effectively for multiple users and utilize the Successive Interference Cancellation (SIC). For increasing the SE, the MA-MIMO is integrated with NOMA, and it is proven that NOMA can enhance the SE significantly when compared to the traditional OMA [9]. In the NOMA system, many users are supported by the SIC and intra-beam superposition. The usage of power domains is carried out for the enhancement of SE with the users and several channel gains [10-12]. Further, due to the advancement of technology, there is a need for high data rates, high SE, and low latency.

The utilization of distributed Access Points (APs) makes the effective spatial resource allocation [13]. But the inter-cell interference is basic in every cell-centric model, and it is becoming a main performance-limiting criterion. For addressing this issue, CF-MA-MIMO-NOMA systems are introduced. CF-MA-MIMO-NOMA is emerging in recent times due to the integration of MA-MIMO and the distributed antenna model, in which the APs are linked to the Central Processing Unit (CPU). This model simultaneously handles a larger number of small users [14]. The Power Allocation (PA) and precoding are carried out in the CPU, and the CF criteria provide high throughput, SE, and EE. The primary aim of this system is to allocate a larger number of spatially distributed APs to allocate different single antenna users in the same frequency and time domain. Hence, every user is considered by every AP, and it does not undergo cell-free. As mentioned earlier, the MA-MIMO-NOMA provides a better potential for supporting large connection requirements of the upcoming generation [15, 16]. Hence, the integration of MA-MIMO-NOMA with CF may provide better performance, and it has become a significant topic of research. The conventional PA models offer accurate computational allocation, but lack in allocating optimal power to the users. In some of the MA-MIMO-NOMA, the users are split into clusters, and the users in intra clusters are split by the SIC. Then, the inter-cluster interference was minimized by the precoding approach. However, these approaches minimized the power efficiency of the system. The optimal power allocation process is carried out by the Adaptive Squirrel Search Optimization (ASSO). This optimizer is selected because this algorithm enhances the convergence speed and performance. Further, this optimizer allocates the users with better Energy Efficiency (EE) and Spectral Efficiency (SE) for providing an efficient strategy for PA.

One of the peculiarities of the suggested CF-MA-MIMO-NOMA system is that it is connected to an adaptive ASSO-based power allocation approach that will simultaneously maximize the spectral efficiency and energy efficiency. The collaboration between distributed access points and intelligent power management is helpful to suppress interference caused by NOMA as well as mitigate the residual error of less-than-perfect successive interference cancellation. Also, the described architecture is resilient to imperfect knowledge of channel state information and is scalable because it avoids centralized control and inflexible distribution of resources. It provides better throughput, fairness, and energy efficiency compared to the current CF-MIMO and MIMO-NOMA designs.

The rest of the work is sorted as follows: Section 2 states the recent literature works based on the CF-MA-MIMO-NOMA networks; Section 3 shows the proposed CE and PA with a mathematical description; Section 4 analyzes the results' implications, and Section 5 ends with a conclusion.

2. Related work

Initial studies on Cell-Free Massive Multiple-Input Multiple-Output (CF-MIMO) systems have focused on reducing energy consumption by joint Power Allocation (PA) and load balancing, namely, of downlink transmit power as well as Access Point (AP) activation number. These methods were very power-saving and less complex algorithms; they did not consider user clustering and interference due to Non-Orthogonal Multiple Access (NOMA) [17]. Machine-learning-based clustering tools were introduced to CF-MIMO-NOMA designs to deal with the lack of adaptive user segmentation, e.g., enhanced K-means. These techniques model intra-cluster pilot contamination, inter-cluster interference, and imperfect Successive Interference Cancellation (SIC) and optimize PA to Spectral Efficiency (SE), but at the cost of the clustering being kept constant [18]. PA investigations without instantaneous Channel State Information (CSI) had used backhaul combining and user grouping to enhance worst-case uplink Signal-To-Interference-Plus-Noise Ratio (SINR), but not joint optimization with learning-based clustering and SE maximization [19]. In millimeter-wave MIMO-NOMA, it was suggested that user grouping based on channel correlation, along with a convex PA model, mitigates interferences; however, the capability to withstand imperfect CSI and dynamic mobility constraints was not quite strong [20]. The MIMO-NOMA architectures using hybrid-pre-coding and employing Simultaneous Wireless Information And Power Transfer (SWIPT) cluster-head selection and an iterative optimization scheme overcame non-convexity but at the cost of prohibitive computational complexity in real-time adaptability [21]. Strategies of fairness-oriented precoding and PA based upon Semi-Definite Relaxation (SDR), Successive Convex Approximation (SCA), and Minimum Mean-Square Error (MMSE)-equivalence provided better balancing of the rates in MIMO-NOMA types of systems; however, the scalability to large antenna-to-user ratios was not quite achieved [22]. Channel capacity was enhanced by the joint choice of user patterns and PA, based on a matching theory, but the system was not adaptable to cell-free topologies and changing traffic patterns [23].

The occurrence of the Concentration-Free Massive MIMO With Non-Orthogonal Multiple Access (CF-MA-MIMO-NOMA) in scenarios where there is a space-correlated Rician fading has been explored with the formulation of closed equations of Spectral Efficiency (SE) and Energy Efficiency (EE). Such analyses have considered imperfect Successive Interference Cancellation (SIC) and pilot contamination; however, the reliance on statistical channel models has limited the generality of the conclusions [24]. In the second research, opportunities realized with the use of NOMA-based coexistence in CF-MA-MIMO architectures involved the opportunistic alignment of interference, which reduced the antenna overhead. The method, however, did not include adaptive power distribution and an innovative clustering algorithm [25]. The third body of work applied the deep-learning approaches, namely, Bidirectional Gated Recurrent Units (Bi-GRU) with ensemble learning models, to perform channel estimation. However, channel estimation was done without any joint resource optimization [26, 27]. However, such systems failed to jointly optimize the clustering, power allocation, and spectral resource allocation [28].

Deep reinforcement learning models that combine improved K-means clustering, DQN-based sub-channel assignment, and DDPG-based power assignment have proven to be able to fast-track convergence rates and scale-up system capacity in millimeter-wave massive MIMO-NOMA systems, although at a high training complexity cost [29]. Through battery optimization of energy harvesting and data transmission in SWIPT-enabled millimeter-wave massive MIMO-NOMA systems, a significant increase in the energy efficiency was realized through the implementation of hybrid precoding schemes and iterative convex optimization, but this methodology did not have an intrinsic adaptability through learning [30]. Hybrid machine-learning/deep-learning frameworks that combine LSTM-based spectrum prediction with attention-driven clustering have managed to increase spectral efficiency at the cost of power consumption. However, they are still not sufficient to implement NOMA-specific interference and power allocation optimization [31]. Detection and channel estimation algorithms received the assistance of deep learning to provide energy and spectral efficiency gains in IoT-based MIMO-NOMA systems; however, power consumption versus scalability trade-offs were still present [32]. Federated meta-reinforcement learning enables quick adaptation of power distribution and sub-band allocation in multi-cell NOMA [33]. Optimization of beamforming and power assignment in IRS-aided massive MIMO networks maximized weighted sum-rate in both perfect and imperfect channel state information conditions, but did not consider NOMA or user-centric clustering [34]. Wavelet-based NOMA schemes with deep learning optimization specifically optimized to user-centric CF-massive MIMO systems have recorded a reduction of bit-error rate and higher sum-rate achievable; nevertheless, the simultaneous optimization of clustering, power allocation, and spectral resource optimization was not achieved [35].

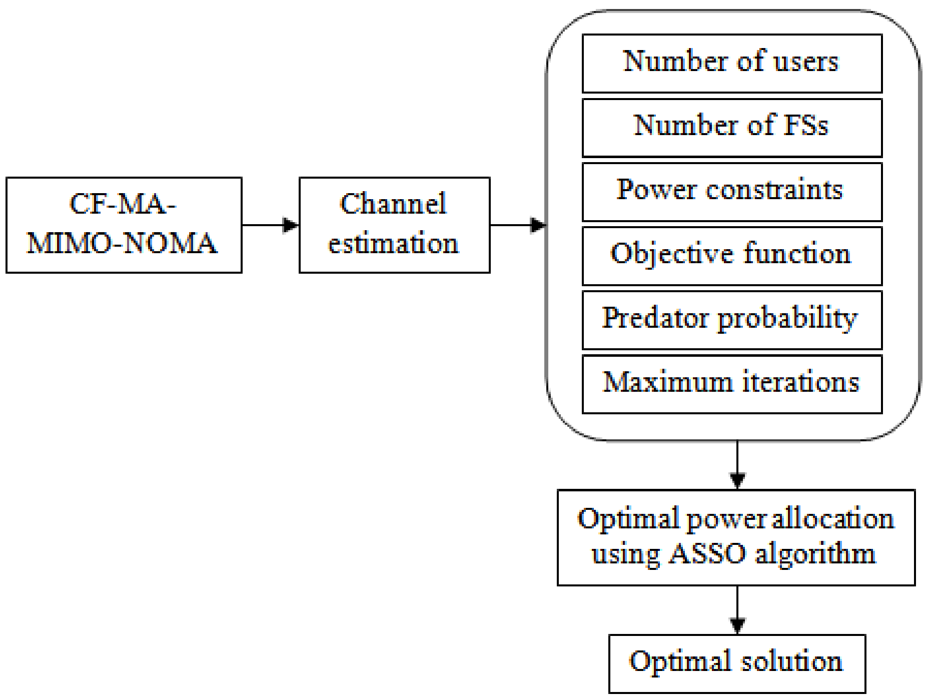

Fig. 1 Workflow of the proposed CF- MA-MIMO-NOMA model ASSO

3. Proposed Method

In this work, CF-MA-MIMO-NOMA, the CE and optimal power allocation are carried out by the EM and ASSO. Figure 1 represents the workflow of the proposed CF-MA-MIMO-NOMA model.

3.1. System Model

In this work, the downlink transmission of CF-MA-MIMO-NOMA and the model Mnumber of APs LN single antenna users are considered. The users are set into Na number of clusters and Lusers $L \geq 2$ per clusters and NOMA is provided between the users. MAntennas and every $AP$are integrated with the CPU through a backhaul link for achieving coherence processing. This model has the payload data, and every APcalculation is performed by the precoder on the basis of the channel medium among the users AP. Figure 2 (a) shows the system model of CF-MA-MIMO-NOMA, and Figure 2 (b) shows the APtransfer to 4 clusters, each of which has 3 users. The downlink medium among the m^{th}_AP is given as$m = 1,2, \ldots\ldots, M$. The l^{th}user$l = 1,2, \ldots\ldots, L$in the n^{th}cluster is represented as $n = 1,2, \ldots\ldots, N$.

$$h_{mnl} \sim cN\left(0, \beta_{mnl} I_Q\right) \tag{1}$$

Where $\beta_{mnl}$is the group of massive scale fading terms, and $h_{mnl} \sim cN(0,1)$ is the small scale fading term.

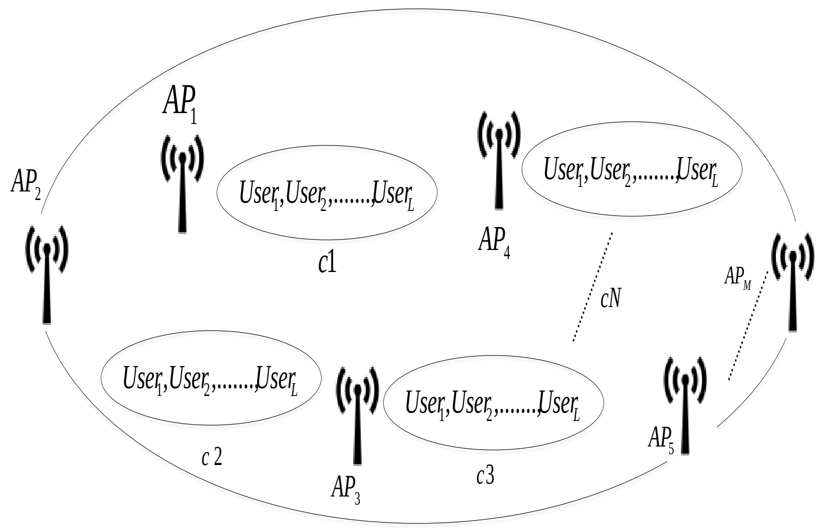

(a)

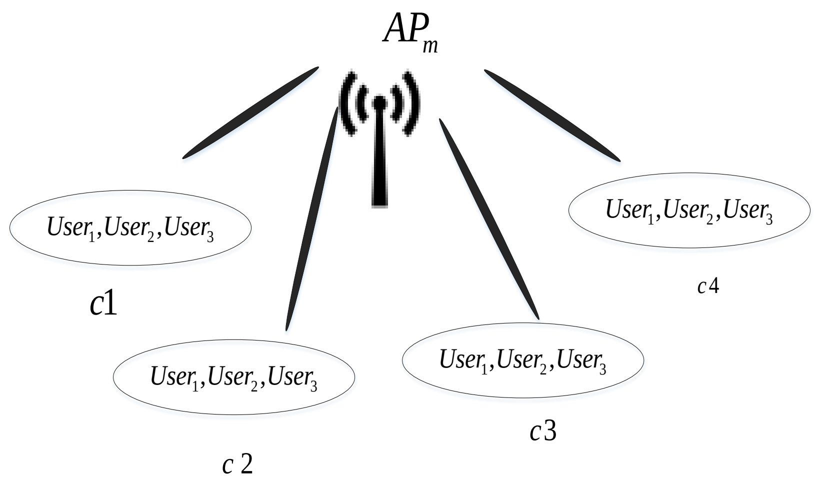

(b)

Fig. 2(a) CF-MA-MIMO-NOMA Model, and (b) AP Transfer to 4-Clusters.

3.2. Downlink Transmission Model

The superposition coding data signal p_{nl} for the l^{th} user having n^{th} a cluster is given as:

$$R_n = \sum_{l=1}^{L} \sqrt{p_{nl}}\, R_{nl}, \quad \forall n \tag{2}$$

Where R_{nl} is the power allocated to the l^{th} user having n^{th} a cluster. Here $p_{nl} = p_t \alpha_{nl}$, in which p_t is the overall power is transmitted to every AP α_{nl} group of power terms. Let the m^{th} AP transmitting the signal is given as:

$$Y_m = \sum_{n=1}^{N} U_{mn} R_n \tag{3}$$

Where U_{mn} is the signal's spatial directivity provided to the user, presented in n^{th} a cluster. The transmitted signals are preceded by a signal AP for every user in a similar cluster. The users LN are distributed at the same time using M a number of APs. During the signal reception, l^{th} a user having n^{th} a cluster is represented as:

$$z_{nl} = \sum_{m=1}^{M} \sqrt{p_{nl}}\, h_{mnl}^{H} U_{mn} R_{nl} + \sum_{m=1}^{M} h_{mnl}^{H} U_{mn} \sum_{i=1}^{L} \sqrt{p_{ni}}\, R_{ni} + \sum_{m=1}^{M} h_{mnl}^{H} \sum_{i=1}^{L} U_{mn'} + \eta_{ml} \tag{4}$$

Where $\sum_{m=1}^{M} \sqrt{p_{nl}}\, h_{mnl}^{H} U_{mn} R_{nl}$ is the desired signal, $\sum_{m=1}^{M} h_{mnl}^{H} U_{mn} \sum_{i=1}^{L} \sqrt{p_{ni}}\, R_{ni}$ and $\sum_{m=1}^{M} h_{mnl}^{H} \sum_{i=1}^{L} U_{mn'} + \eta_{ml}$ are the inter- and intra-cluster interferences. The SIC is transmitted at the receiving side by every user to remove the interferences produced by the users having less gain.

3.3. Channel Estimation

In this work, the CE process is carried out using the EM. The EM is the iterative approach for finding Maximum Likelihood (ML) parameter estimation. There are two stages carried out in the EM: (i) expectation of the Log Likelihood (LL) implemented by the present parameter estimation, and (ii) maximization of the LL obtained in the expectation stage for computing variables. Let the receiving signal have the j^{th} subcarrier given as:

$$z_j = y_j B_j \alpha + u_j \tag{5}$$

Where y_j is the transmitting signal, B_j is the fundamental matrix, α is the basic *coefficient*, and u_j is the Gaussian noise. Hence, the conditional Probability Density Function (PDF) is represented as:

$$f(z_j|y_j;\alpha) = \frac{1}{\pi\sigma_u^2} exp\left\{-\frac{|z_j - y_j B_j \alpha|^2}{\sigma_u^2}\right\} \tag{6}$$

Where σ_u^2 is the variance. When there are G feasible transmitting symbol values, and y_g the transmitting symbols are. Joint-PDF is summed with the $f(z_j y_g;\alpha)$ entire y_g , and the PDF of z_j is computed as:

$$f(z_j;\alpha) = \sum_{y_g} f(z_j y_g;\alpha) \tag{7}$$

$$f(z_j|y_j;\alpha) = \frac{1}{G\pi\sigma_u^2} \sum_{y_g} exp\left\{-\frac{|z_j - y_j B_j \alpha|^2}{\sigma_u^2}\right\} \tag{8}$$

The LL of α is given as:

$$L(\alpha) = ln\, f\,(Z;\alpha) = ln\, f\,(z_j;\alpha) \tag{9}$$

$$= -G\pi\sigma_u^2 + ln \sum_{y_g} exp\left\{-\frac{|z_j - y_j B_j \alpha|^2}{\sigma_u^2}\right\} \tag{10}$$

The ML estimation of α is represented as:

$$\hat{\alpha} = \underset{\alpha}{argmax}\ L(\alpha) \tag{11}$$

It is observed that the EM model uses iteration for obtaining ML estimation, and the initial estimate of α by (11) is $\alpha^{(1)}$ and the m^{th} is $\alpha^{(m)}$

(i) E-stage (expectation-stage): Calculate the E-stage of the LL function as:

$$L_B(\alpha|\alpha^{(m)}) = E_{f(Y|Z;\alpha^{(m)})}[ln\, f\,(Z,Y,\alpha)] \tag{12}$$

(ii) M-stage (Maximization-stage): Calculate the variables of further iteration $\alpha^{(m+1)}$ that increase $L_B(\alpha|\alpha^{(m)})$.

$$\alpha^{(m+1)} = \underset{\alpha}{argmax} L_B(\alpha|\alpha^{(m)}) \tag{13}$$

The convergence criterion is given as:

$$|L_B(\alpha^{(m)}) - L_B(\alpha^{(m+1)})| \leq T_h \tag{14}$$

Where T_h is the threshold value. The computation of $L_B(\alpha|\alpha^{(m)})$ is given as:

$$L_B(\alpha \mid \alpha^{(m)}) = \sum_{y_g} f(y_g|z_j;\alpha^{(m)}) - ln(G\pi\sigma_u^2) + \left\{-\frac{|z_j - y_j B_j \alpha|^2}{\sigma_u^2}\right\} \tag{15}$$

3.4. Optimal Power Allocation

The primary aim of the proposed optimal power allocation is to maximize the SE and EE of the model via the proposed optimization model. The ASSO carries out this process. It is an enhanced version of SSO, and it provides better convergence performance when compared to the standard SSO. The ASSO combines the SSO and IWA (Invasive Weed Algorithm). The algorithm takes as inputs the number of users and access points, transmit power constraints, channel information, SE–EE fitness function, population size, predator probability, and maximum iterations.

Unlike conventional optimization techniques and standard SSO, ASSO introduces adaptive reproduction and Lévy flight–based exploration, which helps avoid premature convergence and ensures robustness in non-convex optimization scenarios. The reproduction process in IWA is included with the SSO for improving the convergence performance. This optimizer allocates the power to the users with high efficiency in a better way. For the network to be efficient in the user's optimal allocation on the basis of power with high SE and EE, the fitness of the network should be maximum.

$$F_t = Max(SE, EE) \tag{16}$$

This optimizer mimics the dynamic characteristics of squirrels' locomotion, which is known as sliding. The value of fitness shows the Hickory tree FS_{hnt}^t (optimal food source), the acorn tree FS_{act}^t (typical food), and the normal tree FS_{not}^t (no food source). During the exploration stage, based on the value of fitness, some FS relocate to the optimal and normal food source. During the exploitation stage, the probability of predator occurrence is taken into account. Let us consider that there are l_{several} FS in the forest, and the location of j^{th} squirrel FS is defined by a vector, and it is indicated in a matrix.

$$F_s = \begin{bmatrix} F_{s1,1} & F_{s1,2} & \cdots & \cdots & F_{s1,dim} \\ F_{s2,1} & F_{s2,2} & \cdots & \cdots & F_{s2,dim} \\ \vdots & \vdots & \vdots & \vdots & \vdots \\ \vdots & \vdots & \vdots & \vdots & \vdots \\ F_{sl,1} & F_{sl,2} & \cdots & \cdots & F_{sl,dim}[] \end{bmatrix} \tag{17}$$

Initializing every FS position is represented as:

$$FS_j = \{FS_{LL} + UP(0,1) \times (FS_{UL} - FS_{LL}) \quad (18)$$

Where FS_{LL} FS_{UL} are the lower and upper ranges of j^{th}squirrel. Let us consider that there are M_{several} trees in a forest. The fitness of the position for every FS is measured using the solution vector, and values are set in the matrix below:

$$f = \begin{bmatrix} f_1([F_{s1,1} & F_{s1,2} & \cdots & \cdots & F_{s1,dim} \\ f_2([F_{s2,1} & F_{s2,2} & \cdots & \cdots & F_{s2,dim} \\ \vdots & \vdots & \vdots & \vdots & \vdots \\ \vdots & \vdots & \vdots & \vdots & \vdots \\ f_m([F_{sl,1} & F_{sl,2} & \cdots & \cdots & F_{sl,dim}[] \end{bmatrix} \quad (19)$$

In the proposed ASSO, the reproduction process of IWA is evaluated for producing new-spring. The iteration $\sigma_{iteration}$ is utilized to update the position on three different strategies.

Strategy 1:$\mathrm{FS}_{\mathrm{act}}^{\mathrm{t}}$ The FS on a regular food source (acorn nut tree) is moved to the $\mathrm{FS}_{\mathrm{hnt}}^{\mathrm{t}}$optimal food source (hickory nut tree). When $\mathrm{Rand1} \geq \mathrm{P_{po}}$the offspring of each FS on the $\mathrm{FS}_{\mathrm{hnt}}^{\mathrm{t}}$is computed by:

$$\sigma_{iteration} = \frac{(Iterationm_{max}}{(Iterationm_{max}[(\sigma_I - \sigma_F) + \sigma_F]} \quad (20)$$

Where $Iteration_{max}$is the maximum iteration, $m$is the non-linear deviation, $\sigma_I$is the initial standard deviation, and $\sigma_F$is the final standard deviation.

FS move from position of FS on theFS_{hnt}^{t} is expressed as:

$$FS_{act}^{t+1} = \begin{cases} FS_{act}^{t} + gl_d GL_c (FS_{hnt}^{t} - FS_{act}^{t}) & Rand1 \geq P_{po} \\ random\ position & elsewhere \end{cases} \quad (21)$$

Where$FS_{act}^{t+1}$is the new position of the squirrels, gl_d is the glide distance, $GL_c$is the gliding constant, $Rand1$is the random number, and $P_{po}$is the probability of predator occurrence.

Strategy 2: When $\mathrm{Rand2} \geq \mathrm{P_{po}}$the offspring of each FS on the $\mathrm{FS}_{\mathrm{act}}^{\mathrm{t}}$is computed by Equation (19), and the positions are recomputed. The following expression is used for computing the FS from a no food source relocated to the regular food source $\mathrm{FS}_{\mathrm{not}}^{\mathrm{t}}$to obtain more energy.

$$FS_{not}^{t+1} = \begin{cases} FS_{not}^{t} + gl_d GL_c (FS_{act}^{t} - FS_{not}^{t}) & Rand2 \geq P_{po} \\ random\ position & elsewhere \end{cases} \quad (22)$$

Where FS_{not}^{t} is FS on the no food source (normal tree), and $Rand2$is the random number.

Strategy 3: When $Rand3 \geq P_{po}$the offspring of each FS on the $FS_{hnt}^{t}$is computed by Equation (19). Then, the FS from no food source relocates to the optimal food source, and it is expressed as:

$$FS_{not}^{t+1} = \begin{cases} FS_{not}^{t} + gl_d GL_c (FS_{hnt}^{t} - FS_{not}^{t}) & Rand3 \geq P_{po} \\ random\ position & elsewhere \end{cases} \quad (23)$$

Where $Rand3$is the random number.

The gliding model of FS is stated as the total of the drag force D_f , and the lift L generates the resulting force R.

$$\frac{L}{D_f} = \frac{1}{\tan\phi} \quad (24)$$

Where $\phi$is the gliding angle.

Variation in seasonal monitoring is developed for maintaining the trade-off between the exploration and exploitation capacity. This characteristic is defined as:

$$S_c = \sqrt{\left(FS_{act}^{t} - FS_{hnt}^{t}\right)}^2 \quad (25)$$

During the winter season, the FS randomly relocated to get the best resources, and it is expressed as:

$$FS_{not}^{t} = FS_{lo} + Levy + (FS_{up} - FS_{lo}) \quad (26)$$

Where $Levy$ is the Lévy flight utilized for finding new candidate solutions and enhancing the exploration capacity. The output of the process (Algorithm 1) is the optimal power allocation vector for all users, along with the corresponding maximum SE and EE values, which are used to validate the effectiveness.

Algorithm 1: ASSO for Optimal Power Allocation

Inputs: Number of users, number of Flying Squirrels (FS), Power Constraints, SE–EE objective function, Predator Probability, Maximum Iterations
Output: Optimal Power Allocation Vector Maximizing Spectral Efficiency (SE) and Energy Efficiency (EE)

1 Initialize FS positions randomly within power bounds and classify them as hickory, acorn, or normal trees based on fitness
2 Evaluate SE–EE fitness and identify the best FS (hickory tree)
3 Move FS from acorn to hickory tree using gliding behavior and IWA-based reproduction.
4 Relocate FS from a normal tree to an acorn tree using random displacement.

5	Directly relocate low-fitness FS from the normal tree to the hickory tree.
6	Modify FS movement based on predator occurrence probability.
7	Apply Lévy flight–based relocation during winter to enhance exploration.
8	Recalculate fitness, update FS positions, and retain the best solution
9	Stop at convergence or maximum iteration and output optimal power allocation.

4. Results and Discussion

The following sections ensure experimental analysis and discussion of the proposed CE and optimal power allocation. The simulative analysis is carried out in the MATLAB platform, which has 8GB RAM and a 64-bit operating system. Table 1 shows the simulation parameters utilized for the experimentation process.

Table 1. Simulation parameters

Parameters	Values
No. of transmitting antennas	16
No. of receiving antennas	16
Users	40
No. of AP	100
Coherence time	100
bandwidth	20 MHz
Fading channel	Raleigh fading
Maximum power allocated to clusters	-30 dBm
Length of block	200 symbols

4.1 Evaluating Measures

The evaluation measures, like BER, achievable sum rate, SE, and EE, are computed.

BER: It computes the errors in the receiving bits to the communicating medium and is varied by the synchronization errors, noise, interference, and distortion. It is the proportion of the number of bits received without error, N_E, the Total number of transmitted bits over a measurement interval of time, N_T. Therefore,

$$BER = \frac{N_E}{N_T} \tag{27}$$

Achievable Sum Rate: It is the most widely utilized performance metric for computing the downlink CF-MA-MIMO-NOMA. This measure computes the codes with high maximum error probability.

SE: It computes the mean number of information bits over the communication channel, and it is expressed as:

$$SE = \frac{Throughput}{Bandwidth} \tag{28}$$

EE: It is computed by the number of bits that are transferred realistically per joules, and it is given as:

$$EE = \frac{Throughput}{Power\ consumption} \tag{29}$$

4.2. Comparative Analysis

The performance of the proposed CE and optimal power allocation model is compared with the various methods. The performance of CE is compared with methods like Least Squares (LS) and Minimum Mean Squared Error (MMSE). Further, the performance of the proposed optimal power allocation model is compared with different optimization approaches like SSO, Salp Swarm Algorithm (SSA), and Particle Swarm Optimizer (PSO) with respect to the measures like SE, EE, and achievable sum rate. Figure 3 shows the comparative analysis of CE and the optimal power allocation model of various approaches with respect to the SNR values. Figure 3 evaluates BER performance across SNR values (1–20 dB) for three CE methods. At 20 dB SNR, LS achieves BER = 1.07×10^{-1}, MMSE achieves 2.01×10^{-2}, and the proposed EM-based method achieves 2.75×10^{-3}. The proposed CE demonstrates superior performance, achieving 38.9 times lower error than LS and 7.3 times lower than MMSE, validating its effectiveness for channel estimation in multi-user systems. Figure 4 evaluates the power allocation performance in terms of SE, EE, and achievable sum rate.

At 20 dB SNR, the proposed ASSO scheme attains a spectral efficiency of approximately 12 bits/s/Hz, which is noticeably higher than SSO 10 bits/s/Hz and clearly above the PSO baseline 7.5 bits/s/Hz. At 10 dB SNR, ASSO achieves an energy efficiency of around 2.4 bits/Joule, whereas PSO reaches only about 1.3 bits/Joule, indicating a substantial advantage for the proposed method. These gains arise from the hybrid SSO–IWA design, which combines fast convergence with strong population diversity and global exploration capability, enabling more effective power allocation than conventional swarm optimizers. Figure 5 shows the analysis of BER with respect to users for various approaches.

The performance of CE is compared with methods like LS and MMSE. Here, the number of users considered is 1 to 40 users. It is observed from the graph that when the number of users is increased, the performance of the BER is also increased. Finally, it is proven that the proposed CE attained better BER when compared to the other two conventional approaches. Figure 6 evaluates the impact of user loading on SE, EE, and achievable sum rate for 1–40 users under four power allocation algorithms (ASSO, SSO, SSA, and PSO). As the number of users increases, all three metrics gradually decline because more users share the same radio resources and generate stronger multi-user interference; however, ASSO consistently maintains the highest performance across the entire user range, followed by SSO, SSA, and PSO. At 40 users, ASSO achieves an SE of roughly 2 bits/s/Hz, compared with about 1.8 and 1.6 bits/s/Hz for SSO and SSA, while PSO yields only around 1.4 bits/s/Hz. In terms of energy efficiency at this loading point, ASSO attains approximately 3.8 bits/Joule, whereas SSO, SSA, and PSO provide about 3.5, 3.1, and 2.3 bits/Joule, respectively; the achievable sum rate shows a similar ordering, with ASSO delivering around 3.6 bit/s at 40 users and the competing schemes converging to lower values near 3.3, 3.1, and 2.8 bit/s. These results indicate that ASSO scales more gracefully with user density, preserving higher SE, EE, and sum rate even under heavily loaded conditions, owing to its hybrid SSO–IWA design that maintains population diversity, supports effective global exploration, and still converges rapidly to energy and rate-efficient power allocation patterns in CF-mMIMO NOMA systems.

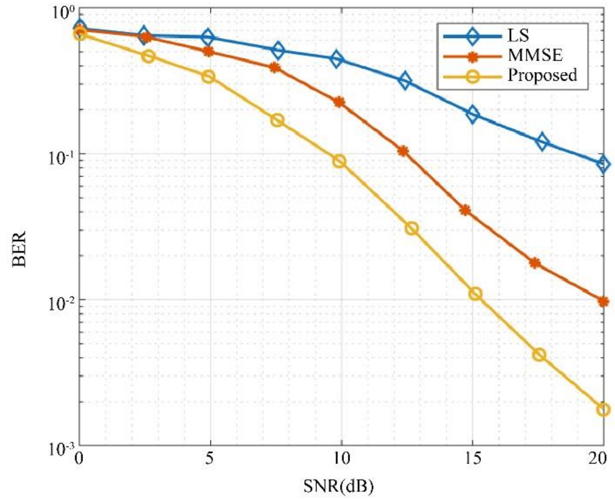

Fig. 3 Analysis of BER with respect to SNR for various approaches

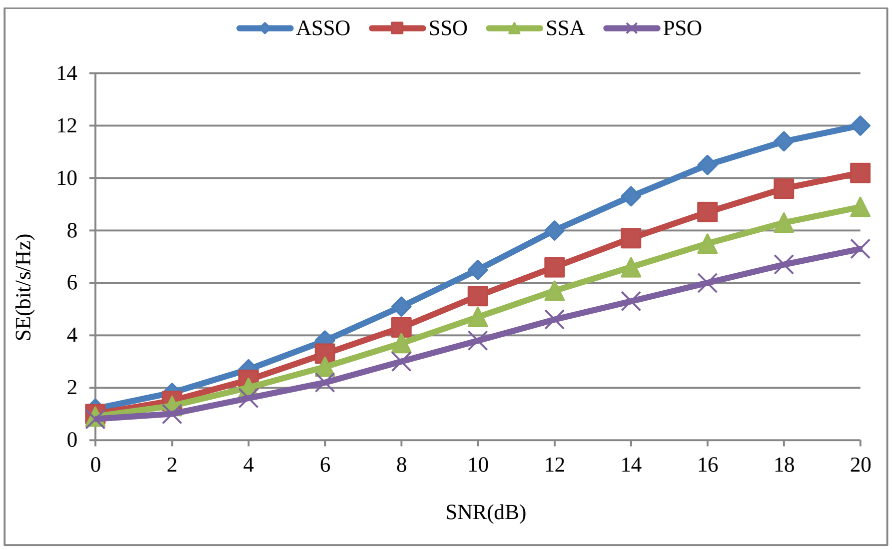

(a)

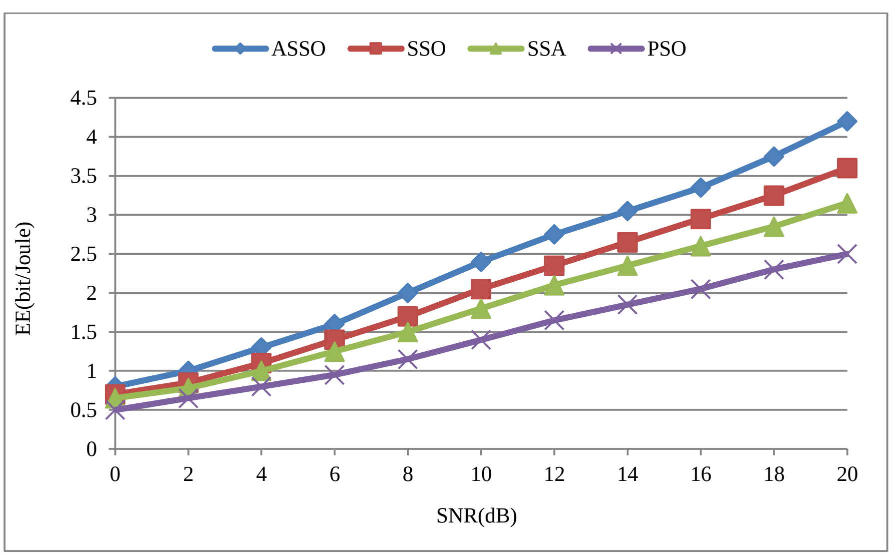

(b)

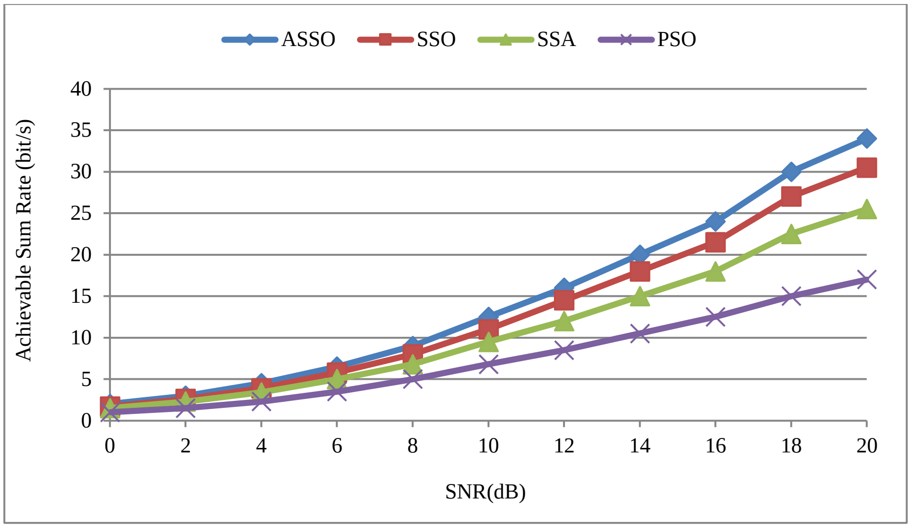

(c)

Fig. 4 Analysis of (a) SE, (b) EE, and (c) Achievable sum rate with respect to SNR For various approaches.

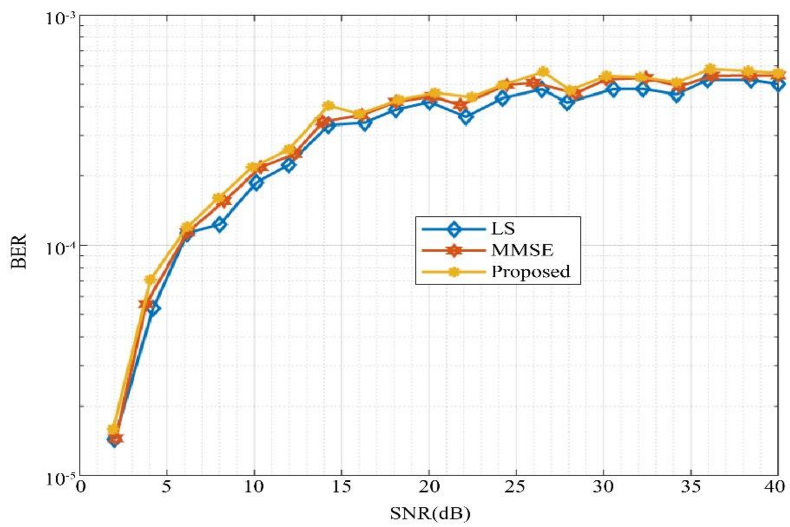

Fig. 5 Analysis of BER with respect to users for various approaches

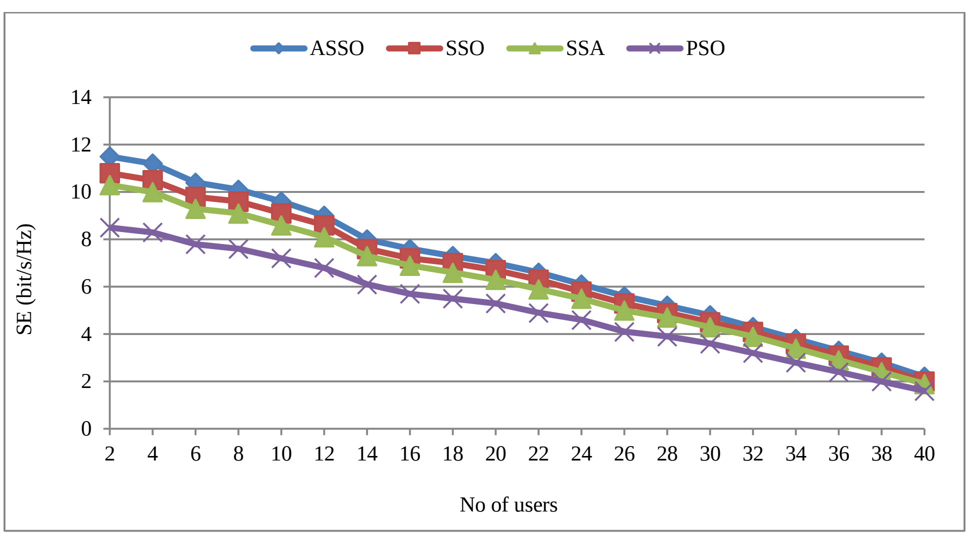

(a)

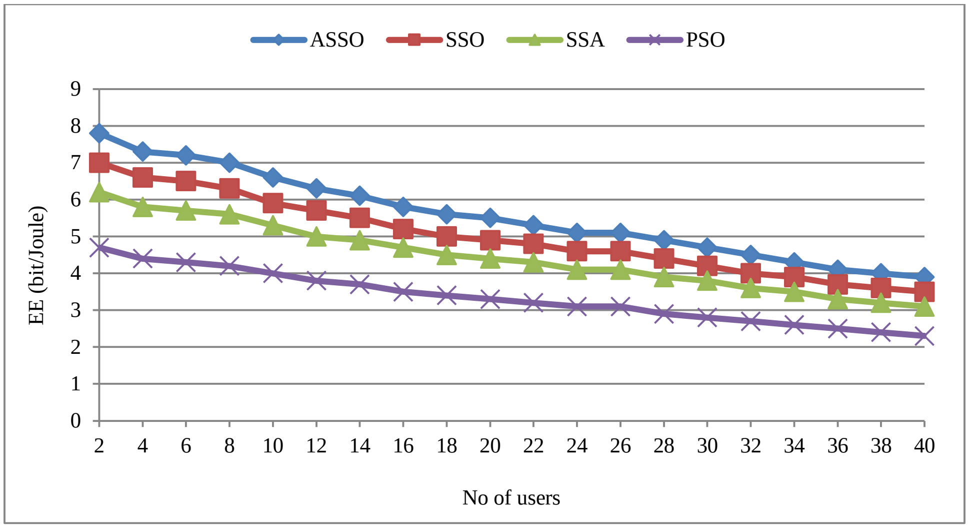

(b)

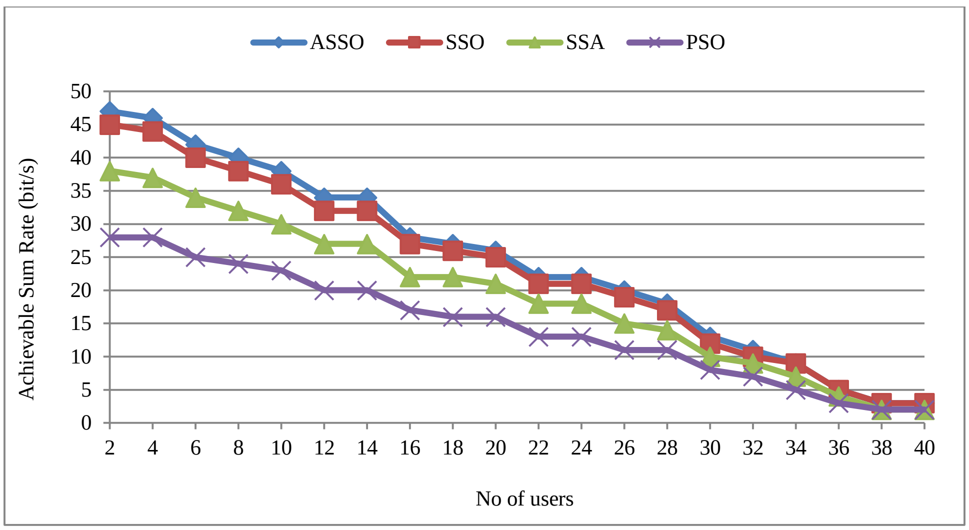

(c)

Fig. 6 Analysis of (a) SE, (b) EE, and (c) Achievable sum.

5. Conclusion

The CF-MA-MIMO-NOMA model with the inclusion of the EM-based channel estimation algorithm and the ASSO-based optimal power allocation algorithm achieves a strong performance improvement in spectral efficiency, energy efficiency, and bit error rate. The model, however, has idealised assumptions of networks and does not take into account highly mobile users, impairment of hardware, and complex inter-cell interference. Moreover, despite the fact that compared to traditional algorithms, ASSO requires fewer computational resources, its complexity can still be a limiting factor in its application to real-time in large-scale networks. Further studies should be conducted on the future of the more advanced deep-learning methods of channel estimation to alleviate estimation error further in dynamically changing conditions. Also, the efficacy and adaptability of power allocation schemes may be enhanced by the utilisation of hybrid or metaheuristic optimisation methods. Expanding the analytical model to integrate a multi-cell, multi-service, and heterogeneous networking environment would provide a more detailed evaluation of system operation in the realistic 5G and beyond environment.

References

[1] Victoria M.T. Palhares, Andre R. Flores, and Rodrigo C. de Lamare, "Robust MMSE Precoding and Power Allocation for Cell-Free Massive MIMO Systems," *IEEE Transactions on Vehicular Technology*, vol. 70, no. 5, pp. 5115-5120, 2021. [CrossRef] [Google Scholar] [Publisher Link]

[2] Yu Zhao, Ignas G. Niemegeers, and Sonia Heemstra De Groot, "Power Allocation in Cell-Free Massive MIMO: A Deep Learning Method," *IEEE Access*, vol. 8, pp. 87185-87200, 2020. [CrossRef] [Google Scholar] [Publisher Link]

[3] Sucharita Chakraborty et al., "Efficient Downlink Power Allocation Algorithms for Cell-Free Massive MIMO Systems," *IEEE Open Journal of the Communications Society*, vol. 2, pp. 168-186, 2021. [CrossRef] [Google Scholar] [Publisher Link]

[4] Naresh Kumar, and Vineet Khandelwal, "Magnetic Border Collie Optimization-based Power Allocation in MIMO-NOMA-Aided Visible Light Communication System," *Journal of Optics*, vol. 52, no. 1, pp. 391-405, 2022. [CrossRef] [Google Scholar] [Publisher Link]

[5] Hongmei Liu et al., "Energy Efficiency Optimization based on Power Allocation in Massive MIMO Downlink Systems," *Symmetry*, vol. 14, no. 6, pp. 1-16, 2022. [CrossRef] [Google Scholar] [Publisher Link]

[6] Yebo Gu, Bowen Huang, and Zhilu Wu, "Power Allocation for Secrecy-Capacity-Optimization-Artificial-Noise Secure MIMO Precoding Systems Under Perfect and Imperfect Channel State Information," *Applied Sciences*, vol. 11, no. 10, pp. 1-24, 2021. [CrossRef] [Google Scholar] [Publisher Link]

[7] Omar Elkharbotly et al., "Optimal Power Allocation in Cooperative MIMO-NOMA with FD/HD Relaying in THz Communications," *2020 9th IFIP International Conference on Performance Evaluation and Modeling in Wireless Networks (PEMWN)*, Berlin, Germany, pp. 1-6, 2020. [CrossRef] [Google Scholar] [Publisher Link]

[8] Qiang Wang, and Zhao Wu, "Beamforming Optimization and Power Allocation for User-Centric MIMO-NOMA IoT Networks," *IEEE Access*, vol. 9, pp. 339-348, 2021. [CrossRef] [Google Scholar] [Publisher Link]

[9] Abdolrasoul Sakhaei Gharagezlou, Mahdi Nangir, and Nima Imani, "Energy Efficient Power Allocation with Joint Antenna and User Selection in Massive MIMO Systems," *Computer Networks*, vol. 216, 2022. [CrossRef] [Google Scholar] [Publisher Link]

[10] Abdolrasoul Sakhaei Gharagezlou et al., "An Energy-Efficient Power Allocation Scheme for Millimeter-Wave MIMO-NOMA Systems," *International Journal of Communication Systems*, vol. 36, no. 1, 2023. [CrossRef] [Google Scholar] [Publisher Link]

[11] Nima Imani et al., "Energy Efficient Power Allocation in MIMO Relaying Systems with the MRT Precoding," *International Journal of Communication Systems*, vol. 36, no. 6, 2023. [CrossRef] [Google Scholar] [Publisher Link]

[12] Abdolrasoul Sakhaei Gharagezlou, and Mahdi Nangir, "Sum Rate Analysis and Power Allocation in Massive MIMO Systems with Power Constraints," *2022 12th International Conference on Computer and Knowledge Engineering (ICCKE)*, Mashhad, Iran, pp. 282-287, 2022. [CrossRef] [Google Scholar] [Publisher Link]

[13] Ming Zeng et al., "Energy-Efficient Power Allocation for MIMO-NOMA with Multiple Users in a Cluster," *IEEE Access*, vol. 6, pp. 5170-5181, 2018. [CrossRef] [Google Scholar] [Publisher Link]

[14] Wanming Hao et al., "Energy-Efficient Power Allocation in Millimeter Wave Massive MIMO with Non-Orthogonal Multiple Access," *IEEE Wireless Communications Letters*, vol. 6, no. 6, pp. 782-785, 2017. [CrossRef] [Google Scholar] [Publisher Link]

[15] Yunxiao Zu, Lin Shao, and Bin Hou, "Joint Beamforming and Power Control for Downlink Multi-Cell Massive MIMO System," *Wireless Personal Communications*, vol. 111, no. 1, pp. 245-266, 2019. [CrossRef] [Google Scholar] [Publisher Link]

[16] Sangtani Meghna, "Hybrid Grey Wolf Optimization and Crow Search Algorithm for Power Allocation in MIMO-NOMA Systems," *Journal of Networking and Communication Systems (JNACS)*, vol. 3, no. 2, pp. 9-17, 2020. [CrossRef] [Google Scholar] [Publisher Link]

[17] Trinh Van Chien, Emil Björnson, and Erik G. Larsson, "Joint Power Allocation and Load Balancing Optimization for Energy-Efficient Cell-Free Massive MIMO Networks," *IEEE Transactions on Wireless Communications*, vol. 19, no. 10, pp. 6798-6812, 2020. [CrossRef] [Google Scholar] [Publisher Link]

[18] Quang Nhat Le et al., "Learning-Assisted User Clustering in Cell-Free Massive MIMO-NOMA Networks," *IEEE Transactions on Vehicular Technology*, vol. 70, no. 12, pp. 12872-12887, 2021. [CrossRef] [Google Scholar] [Publisher Link]

[19] The Khai Nguyen, Ha H. Nguyen, and Hoang Duong Tuan, "Max-Min QoS Power Control in Generalized Cell-Free Massive MIMO-NOMA with Optimal Backhaul Combining," *IEEE Transactions on Vehicular Technology*, vol. 69, no. 10, pp. 10949-10964, 2020. [CrossRef] [Google Scholar] [Publisher Link]

[20] Jinle Zhu et al., "Enhanced User Grouping and Power Allocation for Hybrid mmWave MIMO-NOMA Systems," *IEEE Transactions on Wireless Communications*, vol. 21, no. 3, pp. 2034-2050, 2022. [CrossRef] [Google Scholar] [Publisher Link]

[21] Linglong Dai et al., "Hybrid Precoding-based Millimeter-Wave Massive MIMO-NOMA with Simultaneous Wireless Information and Power Transfer," *IEEE Journal on Selected Areas in Communications*, vol. 37, no. 1, pp. 131-141, 2019. [CrossRef] [Google Scholar] [Publisher Link]

[22] Ahmet Zahid Yalcin, Mustafa Kagan Cetin, and Melda Yuksel, "Max-Min Fair Precoder Design and Power Allocation for MU-MIMO NOMA," *IEEE Transactions on Vehicular Technology*, vol. 70, no. 6, pp. 6217-6221, 2021. [CrossRef] [Google Scholar] [Publisher Link]

[23] Satyasen Panda, "Joint User Patterning and Power Control Optimization of MIMO-NOMA Systems," *Wireless Personal Communications*, vol. 112, no. 4, pp. 2557-2573, 2020. [CrossRef] [Google Scholar] [Publisher Link]

[24] Jiayi Zhang et al., "Performance Analysis and Optimization of NOMA-based Cell-Free Massive MIMO for IoT," *IEEE Internet of Things Journal*, vol. 9, no. 12, pp. 9625-9639, 2022. [CrossRef] [Google Scholar] [Publisher Link]

[25] Zeynab Khodkar, and Jamshid Abouei, "NOMA-Inspired Coexistence Enabling Method in Cell-Free Massive MIMO using Opportunistic Interference Alignment," *Computer Communications*, vol. 191, pp. 285-298, 2022. [CrossRef] [Google Scholar] [Publisher Link]

[26] J. Sofia Priya Dharshini, and P. Deepthi Jordhana, “Optimized NOMA System using Hybrid Coding and Deep Learning-based Channel Estimation,” *Wireless Personal Communications*, vol. 134, no. 3, pp. 1801-1826, 2024. [CrossRef] [Google Scholar] [Publisher Link]

[27] Lassaad Smirani, Leila Jamel, and Latifah Almuqren, “Improving Channel Estimation in a NOMA Modulation Environment based on Ensemble Learning,” *Computer Modeling in Engineering and Sciences*, vol. 140, no. 2, pp. 1315-1337, 2024. [CrossRef] [Google Scholar] [Publisher Link]

[28] Rabia Arshad, Sobia Baig, and Saad Aslam, “User Clustering in Cell-Free Massive MIMO NOMA System: A Learning based and User Centric Approach,” *Alexandria Engineering Journal*, vol. 90, pp. 183-196, 2024. [CrossRef] [Google Scholar] [Publisher Link]

[29] Minghao Wang et al., “Spectrum-Efficient User Grouping and Resource Allocation based on Deep Reinforcement Learning for mmWave Massive MIMO-NOMA Systems,” *Scientific Reports*, vol. 14, no. 1, pp. 1-18, 2024. [CrossRef] [Google Scholar] [Publisher Link]

[30] Walid K. Ghamry, and Suzan Shukry, “Joint Optimization of Energy Harvesting and Data Transmission in SWIPT-Enabled Hybrid Precoding mmWave Massive MIMO-NOMA Systems,” *Cluster Computing*, vol. 28, no. 8, 2025. [CrossRef] [Google Scholar] [Publisher Link]

[31] R. Prameela Devi, and Srilakshmi Aouthu, “Hybrid Machine Learning Framework for Spectrum Prediction and User Clustering in mmWave Massive MIMO-NOMA Systems,” *Wireless Personal Communications*, vol. 142, no. 3-4, pp. 321-354, 2025. [CrossRef] [Google Scholar] [Publisher Link]

[32] Mehdi Izadi et al., “The Performance Optimization of MIMO-NOMA Network with a Developed V-BLAST ZF Approach based on LSTM Deep Learning in Internet of Things,” *Wireless Personal Communications*, vol. 143, no. 1-2, pp. 157-186, 2025. [CrossRef] [Google Scholar] [Publisher Link]

[33] Giang Minh Nguyen, Derek Kwaku Pobi Asiedu, and Ji-Hoon Yun, “Fast Adaptation of Multi-Cell NOMA Resource Allocation Via Federated Meta-Reinforcement Learning,” *Computer Networks*, vol. 272, 2025. [CrossRef] [Google Scholar] [Publisher Link]

[34] Mangqing Guo et al., “Joint Beamforming and Power Allocation in Intelligent Reflecting Surface Assisted Massive MIMO Networks,” *Signal Processing*, vol. 239, 2026. [CrossRef] [Google Scholar] [Publisher Link]

[35] Rabia Arshad et al., “Deep Learning-Driven Multi-User Wavelet NOMA for User Centric Cell-Free Massive MIMO Communications,” *Alexandria Engineering Journal*, vol. 128, pp. 533-543, 2025. [CrossRef] [Google Scholar] [Publisher Link]

[36] Mohit Jain, Vijander Singh, and Asha Rani, “A Novel Nature-Inspired Algorithm for Optimization: Squirrel Search Algorithm,” *Swarm and Evolutionary Computation*, vol. 44, pp. 148-175, 2019. [CrossRef] [Google Scholar] [Publisher Link]